Chapter 13

THE DYNAMICS OF THE RIBOSOME AS INFERRED BY CRYO-EM: INDUCED AND SELF-ORGANIZED MOTIONS

Joachim Frank*

Even though its structure is known to atomic resolution, the ways in which the ribosome accomplishes its tasks in synthesizing proteins are still unknown. The key to an understanding of its dynamics might be found in cryo-electron microscopy of trapped states, and an interpretation of the resultant density maps by "molding" the X-ray structures into them. First results, obtained by application of real-space refinement techniques to cryo-EM maps of complexes in different conformations, indicate a complicated internal reorganization. The question arises as to whether the observed conformational changes accompanying ribosomal function might be predictable based on the architecture of the macromolecular complex. It has indeed been possible to derive one of the principal motions (the ratchet motion) by normal mode analysis of the ribosome represented as a simplified mechanical system.

Keywords: translation, translocation, elongation factor G, elongation factor Tu, molecular machines, real space refinement, normal mode analysis.

*Howard Hughes Medical Institute, Health Research, Inc., Wadsworth Center, Empire State Plaza, Albany, New York 12201-0509.
Email address: <joachim@wadsworth.org>

INTRODUCTION

To date, the ribosome is the most complex biological structure solved to atomic resolution (Ban et al., 2000; Wimberly et al., 2000; Schlünzen et al., 2000; Yusupov et al., 2001). Despite the remarkable achievement of X-ray crystallography that the atomic structures represent, an understanding of the translation process is still beyond our reach, in the absence of detailed knowledge about the ribosome's dynamics.

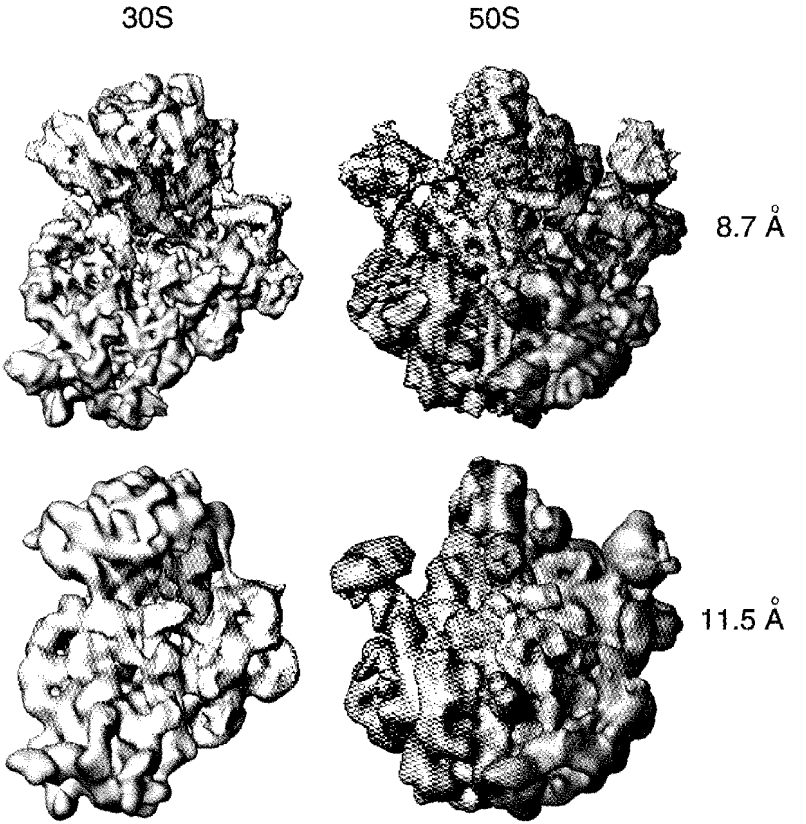

Fig. 1. Cryo-EM maps of 50S large and 30S small subunits of *E. coli* 70S ribosome complexed with fMet-tRNA, reconstructed at two different levels of resolution; the 11.5-Å map (bottom) is obtained from ~73,000 particles (data from Gabashvili *et al.*, 2000), and the 8.7-Å map (top) is obtained from ~110,000 particles using an electron microscope of high stability (from Spahn, Grassucci, Nierhaus, Frank, work in progress).

The entire system formed by the ribosome and its ligands represents a prime example of a molecular machine (see Wilson and Noller, 1998a; Frank, 2000). The technique of cryo-electron microscopy (cryo-EM) and single-particle reconstruction (see Frank, 1996) offers a way to study molecular machines in defined dynamic states, permitting fast immobilization of complexes under conditions closely resembling those found in the living system. The application of cryo-EM to the ribosome is, at the present time, still handicapped by the limited resolution (best resolution to date is 8.7 Å, see Fig. 1; Spahn, Grassucci, Nierhaus, Frank, unpublished; best published structure: 11.5 Å; Gabashvili et al., 2000), and the fact that snapshots of the structure are only available in particular states that have been trapped by the addition of either antibiotics or nonhydrolyzable analogs of GTP. Investigation of other intermediate states must await the development of physical trapping methods, such as spray-freezing (Berriman and Unwin, 1994; White et al., 1998). Nevertheless, even data derived from the more limited studies already allow some important conclusions to be drawn, and some outstanding questions to be formulated with greater insight. On the horizon, as we will see, there is the possibility that dynamic behavior follows "naturally" from properties inherent in the ribosome's architecture.

ELONGATION CYCLE, AND ALTERNATE BINDING OF FACTORS

The elongation cycle of translation (Fig 2) is driven by the alternate binding, to the ribosome, of two molecular complexes with very similar shape: on the one hand, the ternary complex formed by aminoacyl-tRNA, EF-Tu and GTP, and on the other hand, EF-G and GTP. The task of EF-Tu within the ribosome-bound ternary complex is to facilitate decoding and, if a codon-anticodon match is found, subsequent accommodation of the tRNA into the A site. The task of EF-G, once the peptide chain has been elongated and transferred to the new A-site tRNA, is to catalyze the translocation of the complex formed by the two neighboring A- and P-site tRNAs and the mRNA by exactly one codon.

The binding of both key complexes to the ribosome is followed by GTP hydrolysis. The close resemblance between the X-ray structures of

the ternary complex and EF-G•GDP ("molecular mimicry"; Nissen et al., 2000) has led to the suggestion that the two complexes bind to the ribosome in very similar positions. This hypothesis proved to be correct, as was borne out by cryo-electron microscopy (ternary complex: Stark et al., 1997; Agrawal et al., 2000; Valle et al., 2002; EF-G: Agrawal et al., 1998; Stark et al., 2000) and by results from hydroxyl radical probing (EF-G: Wilson and Noller, 1998b). In the cryo-EM maps, we can recognize a complex binding pattern involving several sites on both subunits. In particular, we see the long arm-like domain IV of EF-G reaching into the decoding center, in a way that is quite similar to the approach of the anticodon arm of the tRNA within the ternary complex.

For both the aa-tRNA•EF-Tu•GTP ternary complex and EF-G•GDP, the equivalent sites making contact with the ribosome are known from the results of various cross-linking and footprinting experiments. A careful analysis of these sites in all available X-ray structures (ternary complex: Nissen et al., 1995; Kjeldgaard et al., 1993; Kawashima et al., 1996; Berchtold et al., 1993; Heffron and Jurnak, 2000: EF-G: al-Karadaghi et al., 1996; Æversson et al., 1994; Czworkowski et al., 1994) leads to the conclusion that they form different, non-congruent

Fig. 2. (Figure on facing page)
Elongation cycle of translation. The ribosome is viewed from the "top"; 30S subunit in yellow, 50S subunit in blue. Color scheme for tRNAs: pink, A site; green, P site; brown, E site.

(i.) Deacylated tRNA at the P site, polypeptide linked to tRNA at the A site.

(ii.) EF-G binds to ribosome, followed by GTP hydrolysis, and translocation of tRNA from A- and P- to P- and E- sites.

(iii.) EF-G has exited, and the ribosome is ready for the incorporation of the next tRNA at the A site, as dictated by the next codon.

(iv.) EF-Tu brings a new tRNA to the ribosome. In the decoding step, the anticodon is checked against the codon for match. If correct match is found, a signal is transmitted to the EF-Tu binding sites, GTP hydrolysis ensues, EF-Tu exits, and tRNA is accommodated at the A site. This event is immediately followed by polypeptide transfer from the P- to the A-site tRNA. [Note that the previous version of this diagram depicted a flipped orientation of the E- site tRNA immediately before its removal from the ribosome; the position shown follows from recent evidence (Valle *et al.*, 2003), which shows the outer side of the elbow contacting the L1 stalk]. [Adapted from Frank *et al.*, 2000, and reproduced with permission by ASM Press]

constellations. In other words, it is not possible to superimpose the two molecules such that the corresponding binding sites overlap. (It is true that an atomic structure of EF-G in the form in which it binds the ribosome is still not available, but solution scattering data obtained by Czworkowski and Moore (1997) suggest that it is very similar to the GDP form). From this analysis alone it follows that the ribosome, to accommodate the two ligands in successive phases of the elongation cycle, has to alternate between two different conformations. Thus a simplified description of the sequence of events during the elongation cycle might be as follows:

1. Factor A binds to ribosome in State I
2. GTP hydrolysis

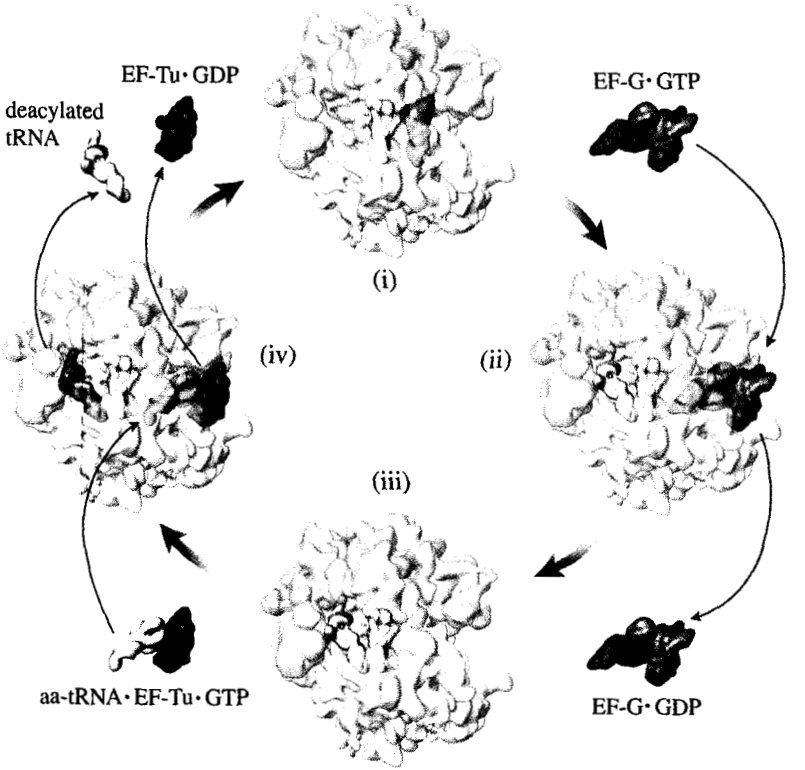

Fig. 2.

3. Ribosome goes into State II, causing release of Factor A
4. Factor B binds to ribosome in State II
5. GTP hydrolysis
6. Ribosome goes into State I, causing release of Factor B
....

This scheme would explain ribosome function during elongation as a chemically driven stochastic two-punch process. Binding of either ligand twice in a row would be automatically prohibited, since the steric requirements would no longer be met in the second attempt. Earlier observations of biochemical properties have indeed led to the concept of two principal states of the ribosome, pre- and post-translocational, which we can equate to the postulated states I and II in above scheme. These two states are separated by a large energy barrier of 120 kJ/mol (Schilling-Bartetzko et al., 1992).

OBSERVED CONFORMATIONAL CHANGES OF THE RIBOSOME

In the course of analyzing numerous cryo-EM maps depicting ribosomes in various ligand binding states, we have observed many changes in the position of components. For example, the top portion of helix 44 of the 16S RNA moves by 8Å during translocation (VanLoock et al., 2000); the double-lobed L7/L12 stalk base is found in different conformations (Rawat et al., 2002); the L1 stalk has been found in different positions related by a flexing of the RNA at its base (Gomez et al., 2000; M. Valle, *et al.*, 2003); and the mRNA channel in the small subunit, at the junction of head and body, opens and closes sideways (Lata et al., 1996), a movement later described as the action of a "latch" (Schlünzen et al., 2000). The most dramatic change observed was a rotation of the small subunit with respect to the large subunit, which occurs in response to the binding of EF-G in the GTP state (Agrawal et al., 1999; Frank and Agrawal, 2000). In the following, this particular motion, referred to as the "ratchet motion," will be analyzed in some detail. This is essentially in continuation of an earlier analysis (Frank and Agrawal, 2002). Special attention will be focused on the extent to which the intersubunit bridges are involved.

The idea has been put forth that the two ribosomal states, associated with alternate factor binding, are in fact related by the ratchet motion (Frank and Agrawal, 2002). Since three of the binding sites are on the small subunit, and another three on the large subunit, a relative rotation of the subunits would indeed produce a series of unique binding constellations. However, closer analysis (M. Valle *et al.*, 2003) has not confirmed this speculation: the ratchet motion as described above is only observed as part of the translocation process, and after the motion the ribosome appears to revert completely, yielding the initial relative subunit orientation, once translocation is complete. Rather, the conformational change that is instrumental for the discrimination between the factors must be a more complex reorganization, affecting the specific geometry of the factor binding region, for instance a change in the intersubunit distance (opening and closing of the intersubunit space) and/or in the structure of the L7/L12 stalk base.

In order to link the observed global changes to local molecular reorganizations, which may constitute the origin of the movement, we need a more quantitative basis for analysis. The observed density maps must be fitted with suitably deformed or reorganized versions of the X-ray structure. The approach that we have chosen is real-space refinement. In this computational approach developed by Chapman (1995), the X-ray structure is cut into components that are likely to be stable units: proteins, either whole or after division into major domains, and high-stability components of RNA such as double-helical regions. Cutting points are chosen to coincide with regions of known instability, or where there is experimental evidence of disorder in the structure. These components are then used to generate electron densities, which are individually fitted into the cryo-EM map. In the end, the underlying substructures are re-linked under observation of stereochemical constraints. In other words, the idea is to mold the X-ray structure into the cryo-EM maps depicting different states of the ribosome structure.

Following a least-squares approach, the residual subject to minimization is formed by two components: one relating to the difference between the observed and the target density maps, the other to the energy of the stereochemical interactions at the structural seams (Chapman, 1995). This kind of analysis was first applied to EM

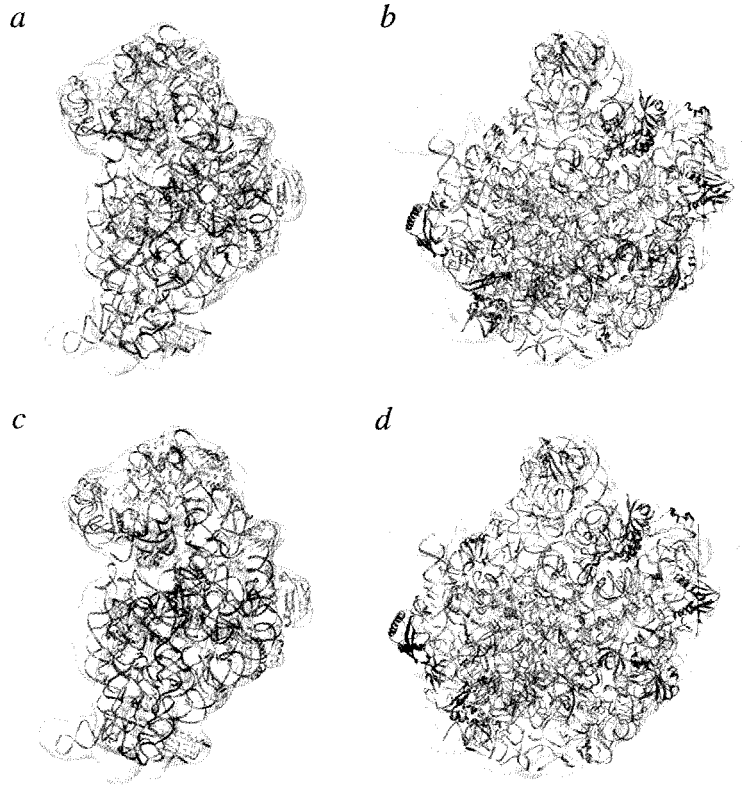

Fig. 3. Interpretation, in terms of the X-ray structure, of cryo-EM density maps of ribosomes in two different conformational states, related by the ratchet motion. Cryo-EM densities are shown as contour maps, displayed in Iris Explorer (Numerical Algorithms Group Inc., Downers Grove, IL). Re-modeled X-ray structures, using real-space refinement, are displayed as ribbon diagrams (Carson, 1997).

reconstructions of insect flight muscle, which were interpreted in terms of actin-myosin interactions in different constellations (Chen et al., 2001). The approach is not without its problems: all of the strain in the change of the structure has to be absorbed by the bonds at the sites where the structure is broken up and then mended. Nevertheless, by using a large number of pieces (over 160 in our case), we can at least approximate an even distribution of strain over the whole molecule.

This analysis has been applied to several maps that depict the extreme positions of the ratchet motion (Gao, *et al.*, 2003). In the first

step, the X-ray structures of both the 30S and 50S subunits were modified to account for the species-dependent variations of ribosomal RNA. Proteins were homology-modeled on the basis of sequence similarity between *E. coli* proteins and their counterparts from the other prokaryotic species for which the X-ray coordinates are known (*Haloarcula marismortui* (Ban et al., 2000), *Thermus thermophilus* (Wimberly et al., 2000; Yusupov et al., 2001), and *Deinococcus radiodurans* (Harms et al., 2001)). The remodeled X-ray structures were then separately fitted, using real-space refinement, into the 70S density map.

The quality of the fits can be characterized by three measures: correlation coefficient, real-space R-factor, and number of van der Waals contact violations. For both of the subunits, values of 0.7, 0.25, and ~3000 are typical for these measures, respectively. The quality of the fits can be seen from a display in which the cryo-EM density is shown as a contour, while the remodeled X-ray structure is represented as a ribbon diagram (Fig. 3). An animated 3D display of the structure, alternating between the two conformations, is particularly useful in the interpretation (See enclosed CD). A preliminary analysis yields the following results:

1) The apparent center of the ratchet rotation lies in helix 27 of the 16S rRNA. Known as the switch helix, this structure changes its conformation in the decoding process following a local reorganization of secondary structure (Lodmell and Dahlberg, 1997), which in turn affects the conformation of the whole ribosome (Gabashvili et al., 1999).
2) Several proteins change their positions drastically. Perhaps some of these changes may bring about changes in system behavior by "mechanical shunting" (see the discussion on normal mode analysis below).
3) The 16S rRNA of the small subunit changes from a compact to a looser configuration. One of the effects of this "breathing" movement is the opening of the entrance and exit channels known to conduct the mRNA. Indeed, an open state of the channels would be required for the mRNA to move, during translocation, while a clamped-close state would be of benefit during the decoding process since this would convey maximum stability to the mRNA (Frank and Agrawal, 2000).

4) The largest structural reorganization occurs in the region of the intersubunit bridges connecting the central protuberance of the large subunit with the head of the small subunit.

TOWARD AN UNDERSTANDING OF RIBOSOME DYNAMICS

In the seeking of metaphors to explain the mechanism of ribosomal action, the three images that come to mind are a clock, a Rube Goldberg mechanism, and a guitar. Although the *clockwork* mechanism has been invoked, in jest, in a review on ribosome functions (Staehelin et al., 1967; Fig. 4), it is clear that a deterministic, gear-like mechanism will not suffice as an explanation, since stochastic processes are inevitably involved at molecular dimensions. *Rube Goldberg's* devices are characterized by elaborate, indirect pathways of action grafted onto devices originally designed for a much simpler purpose (see Berry, 2001). The reason why this image comes to mind is that a number of long cause-and-effect routes have by now been discovered in the ribosome, requiring an ever-increasing complexity of conformational signaling as an explanation. The ribosome might be viewed as an essentially rigid structural framework that requires a large number of additional interacting levers, as in a Rube Goldberg invention, to bring about complex motions. The *guitar*, finally, might be an apt metaphor for an architecture that supports certain modes of motion based on its very design. This last idea has a strong appeal and plausibility: could the

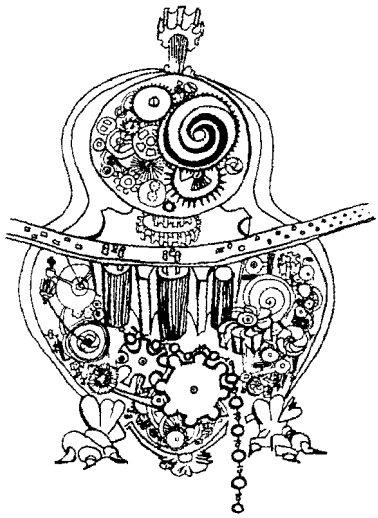

Fig. 4. The ribosome conceived as a clockwork mechanism; from Staehelin et al., (1967), reproduced with permission from Academic Press.

various motions of the ribosome be explained on the basis of its architecture?

To approach this question, the ribosome structure was subjected to normal mode analysis (F. Tama *et al.*, 2003). In this analysis, the atomic structure of a molecule is modeled in a simplified way as a system of masses connected with springs (Hooke's Law) to represent their interactions. The mathematical analysis of the resulting equation system leads to an eigenvector problem that can be solved by standard matrix inversion techniques. However, the unusual size of the problem – originally over 100,000 atoms in the ribosome – necessitated a number of simplifications and approximations.

Normal mode analysis yields a set of eigenmodes, which are collective motions of the pseudo-atoms, characteristic for the ways in which they are connected in the structure under consideration and for the way in which the entire structure is shaped. The modes are mutually orthogonal, ranked by importance, and form a complete, orthonormalized system. Thus, any actual motion of the structure can be uniquely represented by a linear superposition of these modes.

This analysis was applied to the coordinates of the ribosome from *Thermus thermophilus* (Yusupov et al., 2001). Since only motions affecting whole domains are of interest, it is sufficient here to use the phosphate groups to model RNA and C_α atoms to model the proteins.

Remarkably, the high-ranking modes, representing a relatively large share of the total energy, are very similar to the motions experimentally observed. In them, the small subunit is seen to perform a ratchet rotation around an axis that coincides with helix 27, and the L1 stalk swivels between two positions, one in which it blocks the intersubunit space, and the other in which it leaves the space open. This particular mode is quite similar to the motion observed for the post-termination complex (Valle *et al.*, 2003). Other modes show movements that have also been inferred from previous experimental work, such as the swinging motion of the C-terminal domain of protein L9 (Matadeen et al., 1999) and the variation in the spacing between the subunits.

We have thus a sketchy beginning of a possible summary explanation of ribosomal dynamics: energy supplied by thermal motion, by GTP hydrolysis, and by ligand binding could be channeled into

discrete, unique motions that are preferred, based on how the structure is configured at the time when the energy is supplied. [It is necessary to use this general formulation "the way the structure is configured at the time ..." instead of "the way the structure is built," since this formulation allows for the switching of the dynamical properties, or mode preferences.] Changes in configuration, and hence in dynamic properties, could be introduced by the switching of bi-stable RNA secondary structure elements (example: helix 27) or could be due to changes in protein-protein contacts (example: the S13-L5 contacts in the bridges between the central protuberance of the large subunit and the head of the small subunit). It is this possibility of switching that may be able to combine the multifaceted patterns of ribosome dynamics observed thus far into a single, unifying picture.

CONCLUSION

Although "snapshot" evidence collected by cryo-EM of ribosomal conformations determined by antibiotic binding or inhibition of GTP hydrolysis is rather sparse and anecdotal, it has shown that the ribosome undergoes dramatic changes during its functional cycle. We have demonstrated that a method of real-space refinement can be used to obtain atomic models of the ribosome in the alternate conformations, essentially by molding the X-ray structure into the various cryo-EM maps. A careful analysis of such models is expected to yield clues to the local conformational changes underlying the global reorganizations of the ribosome. Finally, we now have evidence that at least some of the motions inferred from the observed conformational changes can be explained on the basis of the properties of the complex mechanical system as a whole. Surely, this is just the beginning of a long voyage toward the discovery of one of life's most intriguing mysteries.

ACKNOWLEDGEMENTS

I thank Michael Watters for assistance with the illustrations, and Adriana Verschoor for a critical reading of the manuscript. This work was

supported by the Howard Hughes Medical Institute and NIH grants R37 GM29169, R01 GM55440, and P41 RR01219.

REFERENCES

1. Ævarsson A, Brazhnikov E, Garber M, Zheltonosova J, Chirgadze Y, al-Karadaghi S, Svensson LA, Liljas A. Three-dimensional structure of the ribosomal translocase: elongation factor G from *Thermus thermophilus*. *EMBO J*, 1994; **13**: 3669-3677.
2. Agrawal RK, Penczek P, Grassucci RA, Frank J. Visualization of elongation factor G on the *Escherichia coli* 70S ribosome: the mechanism of translocation. *Proc Natl Acad Sci USA*, 1998; **95**:6134-6138.
3. Agrawal RK, Heagle AB, Penczek P, Grassucci RA, Frank J. EF-G-dependent GTP hydrolysis induces translocation accompanied by large conformational changes in the 70S ribosome. *Nature Struct Biology*, 1999; **6**:643-647.
4. Agrawal RK, Heagle B, Frank J. Studies of Elongation factor G-dependent tRNA translocation by three-dimensional cryo-electron microscopy. In *The Ribosome: Structure, Function, Antibiotics, and Cellular Interactions*, Edited by R.A. Garrett, S.R. Douthwaite, A. Liljas, A.T. Matheson, P.B. Moore, and H.F. Noller, ASM Press, Washington, DC, 2000, pp53-62.
5. al-Karadaghi S, Ævarsson A, Garber M, Zheltonosova J, Liljas A. The structure of elongation factor G in complex with GDP: conformational flexibility and nucleotide exchange. *Structure*, 1996; **4**: 555-565.
6. Ban N, Nissen P, Hansen J, Moore PB, Steitz TA. The complete atomic structure of the large ribosomal subunit at 2.4 Å resolution. *Science*, 2000; **289**: 905-920.
7. Berchtold H, Reshetnikova L, Reiser CO, Schimer NK, Sprinzl M, Hilgenfeld R. Crystal structure of active elongation factor Tu reveals major domain rearrangements. *Nature*, 1993; **365**: 126-132.
8. Berry I. *Chain Reaction*, Tang Teaching Museum and Art Gallery at Skidmore College, Saratoga Springs, NY, 2001.
9. Berriman J, Unwin N. Analysis of transient structures by cryo-microscopy combined with rapid mixing of spray droplets. *Ultramicroscopy*, 1994; **56**: 241-252.
10. Carson M. Ribbons. *Methods Enzymol*, 1997; **277**: 493-505.

11. Chapman MS. Restrained real-space macromolecular atomic refinement using a new resolution-dependent electron-density function. *Acta Cryst,*1995; **A51**: 69-80.
12. Chen LF, Blanc E, Chapman MS, Taylor K. Real space refinement of Acto-myosin structures from sectioned muscle. *J Struct Biol*, 2001; **133**: 221-232.
13. Czworkowski J, Moore PB. The conformational properties of elongation factor G and the mechanism of translocation. *Biochem*, 1997; **36**: 10327-10334.
14. Czworkowski J, Wang J, Steitz TA, Moore PB. The crystal structure of elongation factor G complexed with GDP, at 2.7 Å resolution. *EMBO J*, 1994; **13**: 3661-3668.
15. Frank J. Three-dimensional Electron Microscopy of Macromolecular Assemblies. Academic Press, San Diego, 1996.
16. Frank J. The ribosome – a macromolecular machine par excellence. *Chem & Biol*, 2000; **7**: R133-R141.
17. Frank J, Agrawal RK. A ratchet-like inter-subunit reorganization of the ribosome during translocation. *Nature*, 2000; **406**: 318-322.
18. Frank J et al. Cryo-electron microscopy of the translational apparatus: Experimental evidence for the paths of mRNA, tRNA, and the polypeptide chain, in RA Garrett, SR Douthwaite, A Liljas, AT Matheson, PB Moore, and HF Noller (eds.), *The Ribosome: Structure, Function, Antibiotics, and Cellular Interactions*, ASM Press, Washington, DC, 2000, pp. 45-51.
19. Frank J, Agrawal RK. Ratchet-like movements between the two ribosomal subunits: their implications in elongation factor recognition and tRNA translocation, in *Cold Spring Harbor Symposia on Quantitative Biology: The Ribosome*, Cold Spring Harbor Press, NY, 2002, p67-75.
20. Gabashvili IS, Agrawal RK, Grassucci R, Squires CL, Dahlberg AE, Frank J. Major rearrangements in the 70S ribosomal 3D structure caused by a conformational switch in 16S ribosomal RNA. *EMBO J*, 1999; **18**: 6501-6507.
21. Gao H, Sengupta J, Valle M, Korostelev A, Eswar N, Stagg SM, Van Roey P, Agrawal RK, Harvey SC, Sali A, Chapman MS, Frank J. Study of the structural dynamics of the *E. coli* 70S ribosome using real space refinements. *Cell*, 2003; **113**: 789-801.
22. Gabashvili IS, Agrawal RK, Spahn CMT, Grassucci RA, Svergun DI, Frank J, Penczek P. Solution structure of the *E. Coli* ribosome at 11.5 Å resolution. *Cell*, 2000; **100**: 51-63.

23. Gomez-Lorenzo MG, Spahn CMT, Agrawal RK, Grassucci RA, Penczek P, Chakraburtty K, Ballesta JPG, Lavandera JL, Garcia-Bustos JF, Frank J. Three-dimensional cryo-electron microscopy localization of EF2 in the *Saccharomyces cerevisiae* 80S ribosome at 17.5 Å resolution. *EMBO J*, 2000; **19**: 1-10.
24. Harms J, Schlünzen F, Zarivach R, Bashan A, Gat S, Agmon I, Bartels H, Franceshi F, Yonath A. High resolution structure of the large ribosomal subunit from a mesophilic eubacterium. *Cell*, 2001; **107**: 679-688.
25. Herron SR, Jurnak F. Structure of an EF-Tu complex with a thiazolyl peptide antibiotic determined at 2.35 Å resolution: atomic basis for GE 2270A inhibition of EF-Tu. *Biochem*, 2000; **39**: 37-45.
26. Kawashima T, Berthet-Colominas C, Wulff M, Cusack S, Leberman R. The structure of the *Escherichia coli* EF-Tu-EF-Ts complex at 2.5 Å resolution. *Nature*, 1996; **379**: 511-518.
27. Kjeldgaard M, Nissen P, Tirup S, Nyborg J. The crystal structure of elongation factor EF-Tu from *Thermus aquaticus* in the GTP conformation. *Structure*, 1993; **1**: 35-50.
28. Lata KR, Agrawal RK, Penczek P, Grassucci R, Zhu J, Frank J. Three-dimensional reconstruction of *Escherichia coli* 30S ribosomal subunit in ice. *J Mol Biol,* 1996; **262**: 43-52.
29. Lodmell JS, Dahlberg AE. A conformational switch in *Escherichia coli* 16S ribosomal RNA during decoding of messenger RNA. *Science*, 1997; **277**: 1262-1267.
30. Matadeen R, Patwardhan A, Gowen B, Orlova EV, Mueller F, Brimacombe R, van Heel M. The *Escherichia coli* large ribosomal subunit at 7.5 Å resolution. *Structure*, 1999;**7**;1575-1583.
31. Nissen P, Kjeldgaard M, Thirup S, Polekhina G, Reshetnikova L, Clark BFC, Nyborg J. Crystal structure of the ternary complex of Phe-tRNA^{Phe}, EF-Tu, and a GTP analog. *Science*, 1995; **270**: 1464-1472.
32. Nissen P, Kjeldgaard M, Nyborg J. Macromolecular mimicry. *EMBO J.*, 2000; **19**: 489-495.
33. Rawat UBS, Zavialov AV, Sengupta J, Valle M, Grassucci RA, Linde J, Vestergaard B, Ehrenberg M, Frank J. A cryo-electron microscopic study of ribosome-bound termination factor RF2, Nature submitted, 2002.
34. Schilling-Bartetzko S, Bartetzko A, Nierhaus KH. Kinetic and thermodynamic parameters for tRNA binding to the ribosome and for the translocational reaction. *J Biol Chem*, 1992; **267**: 4703-4712.

35. Schlünzen F, Tocilj A, Zarivach R, Harms J, Glühmann M, Janell D, Bashan A, Bartels H, Agmon I, Franceschi F, Yonath A. Structure of functionally activated small ribosomal subunit at 3.3 Å resolution. *Cell*, 2000; **102**: 615-623.
36. Staehelin T et al. in Vogal H J, Lampen J O and Bryson V (eds.), *Organizational Biosythesis*, Academic Press, San Diego, CA, 1967, pp. 443-457.
37. Stark GH, Rodnina MV, Wieden HJ, van Heel M, Wintermeyer W. Large-scale movement of elongation factor G and extensive conformational change of the ribosome during translocation. *Cell*, 2000; **100**: 301-309.
38. Stark H, Rodnina M, Rinkeappel J, Brimacombe R, Wintermeyer W, van Heel M. Visualization of elongation factor Tu on the *Escherichia coli* ribosome. *Nature*, 1997; **389**: 403-406.
39. Tama F, Valle M, Frank J, Brooks Ill, CL. Dynamic reorganization of ribosome explored by normal mode analysis and cryo-electron microscopy. *Proc Natl Acad Sci (USA)*, 2003; **100**: 9319-9323.
40. Valle M, Sengupta J, Swami NK, Grassucci RA, Burkhardt N, Nierhaus KH, Agrawal RK, Frank J. Cryo-EM reveals an active role for aminoacyl-tRNA in the accommodation process. *EMBO J*, 2002; **21**: 3557-3567.
41. Valle M, Zawialov A, Sengupta J, Rawat U, Ehrenberg M, Frank J. Locking and unlocking of ribosomal motions. *Cell*, 2003; **114**: 123-134.
42. VanLoock MS, Agrawal RK, Gavashvili IS, Qi L, Frank J, Harvey SC. Movement of the decoding region of the 16S ribosomal RNA accompanies tRNA translocation. *J Mol Biol*, 2000; **304**: 507-515.
43. White HD, Walker ML, Trinick J. A computer controlled spraying-freezing apparatus for millisecond time-resolution electron cryomicroscopy. *J Struct Biol*, 1998; **121**: 306-313.
44. Wilson KS, Noller HR. Molecular Movement inside the translational engine. *Cell*, 1998a; **92**: 337-349.
45. Wilson KW, Noller HF. Mapping the position of EF-G in the ribosome by directed hydroxyl radical probing. *Cell*, 1998b; **92**: 131-139.
46. Wimberly BT, Brodersen DE, Clemons WM. Jr, Morgan-Warren RJ, Carter AP, von Rhein C, Hartsch T, Ramakrishnan V. Structure of the 30S ribosomal subunit. *Nature*, 2000; **407**: 327-339.
47. Yusupov, MM, Yusupova GZ, Baucom A, Lieberman K, Earnest TN, Cate JN, Noller HF. Crystal structure of the ribosome at 5.5 Å resolution.